Inorg. Chem. **2002**, *41*, 331–341

Strongly Coupled Porphyrin Arrays Featuring Both π-Cofacial and Linear-π-Conjugative Interactions

James T. Fletcher and Michael J. Therien*

Department of Chemistry, University of Pennsylvania, Philadelphia, Pennsylvania, 19104-6323

Received August 13, 2001

A combination of metal-catalyzed cross-coupling and metal-templated cycloaddition reactions have been utilized to establish multiporphyrin compounds 5-(5′-[15′,15″-bis(10″,20″-di[4-(3-methoxy-3-methylbutoxy)phenyl]porphinato)-zinc(II)]ethyne)-6-[(5‴-10‴,20‴-di[4-(3-methoxy-3-methylbutoxy)phenyl]porphinato)zinc(II)]indane (**1**) and 5,6-bis-(5′-15′,15″-bis[(10′,20′-di[4-(3-methoxy-3-methylbutoxy)phenyl]porphinato)zinc(II)]ethyne)indane (**2**). Compounds **1** and **2** feature a covalently bridged cofacial bis(porphinato)metal core; ethyne bridging moieties conjugate directly one and two respective peripheral (porphinato)zinc(II) substituents to the macrocyclic framework of their corresponding face-to-face porphyrin units. Optical spectroscopy and electrochemical studies demonstrate substantive electronic interactions between the porphyrin subunits of these compounds. Notably, structural and ^{1}H NMR analyses verify that **1** and **2** possess open conformations necessary for binding small molecules within their respective cofacial (porphinato)metal cores.

Introduction

(Porphinato)metal species bearing metal complexes[1−8] or other redox active entities[9,10] as macrocycle substituents have been examined for their potential utility as multielectron oxidation and reduction catalysts. In these systems, the porphyrin-pendant substituents are envisaged to serve as electron reservoirs or sinks, delivering or removing multiple electrons from the focal catalytic unit during substrate turnover. While the utility of such assemblies has been demonstrated,[1,2,4,9,11] in practice, less than optimal electronic coupling between the redox active moieties and the catalytic core often limits the catalytic effectiveness of these supramolecular species.

With respect to small molecule activation, the cofacial (porphinato)metal structural motif[12−14] has shown particular catalytic efficacy in a wide range of multielectron redox transformations.[15−24] This catalytic diversity derives from both the rich coordination chemistry of redox-active metalloporphyrin compounds, and the ease at which appropriate metal−metal distances can be accommodated in such structures. We report herein new archetypes that feature substantial conjugation expansion of the classic cofacial bis-

* To whom correspondence should be addessed. E-mail: herien@a.chem.upenn.edu.

(1) Shi, C.; Anson, F. C. *Inorg. Chem.* **1992**, *31*, 5078−5083.
(2) Anson, F. C.; Shi, C.; Steiger, B. *Acc. Chem. Res.* **1997**, *30*, 437−444.
(3) Yu, H.-Z.; Baskin, J. S.; Steiger, B.; Anson, F. C.; Zewail, A. H. *J. Am. Chem. Soc.* **1999**, *121*, 484−485.
(4) Chan, R. J. H.; Su, Y. O.; Kuwana, T. *Inorg. Chem.* **1985**, *24*, 3777−3784.
(5) Schmidt, E. S.; Calderwood, T. S.; Bruice, T. C. *Inorg. Chem.* **1986**, *25*, 3718−3720.
(6) Araki, K.; Toma, H. E. *Inorg. Chim. Acta* **1991**, *179*, 293−296.
(7) Burrell, A. K.; Campbell, W. M.; Officer, D. L.; Scott, S. M.; Gordon, K. G.; McDonald, M. R. *J. Chem. Soc., Dalton Trans.* **1999**, 3349−3354.
(8) Rhee, S. W.; Na, Y. H.; Do, Y.; Kim, J. *Inorg. Chim. Acta* **2000**, *309*, 49−56.
(9) Barley, M. H.; Rhodes, M. R.; Meyer, T. J. *Inorg. Chem.* **1987**, *26*, 1746−1750.
(10) Rieder, A.; Krautler, B. *J. Am. Chem. Soc.* **2000**, *122*, 9050−9051.
(11) Shi, C.; Anson, F. C. *J. Am. Chem. Soc.* **1991**, *113*, 9564−9570.
(12) Collman, J. P.; Elliott, C. M.; Halbert, T. R.; Tovrog, B. S. *Proc. Natl. Acad. Sci. U.S.A.* **1977**, *74*, 18−22.
(13) Chang, C. K.; Kuo, M.-S.; Wang, C.-B. *J. Heterocycl. Chem.* **1977**, *14*, 943−945.
(14) Kagan, N. E.; Mauzerall, D.; Merrifield, R. B. *J. Am. Chem. Soc.* **1977**, *99*, 5484−5486.
(15) Collman, J. P.; Denisevich, P.; Konai, Y.; Marrocco, M.; Koval, C.; Anson, F. C. *J. Am. Chem. Soc.* **1980**, *102*, 6027−6036.
(16) Chang, C. K.; Liu, H. Y.; Abdalmuhdi, I. *J. Am. Chem. Soc.* **1984**, *106*, 2725−2726.
(17) Liu, H.-Y.; Abdalmuhdi, I.; Chang, C. K.; Anson, F. C. *J. Phys. Chem.* **1985**, *89*, 665−670.
(18) Naruta, Y.; Maruyama, K. *J. Am. Chem. Soc.* **1991**, *113*, 3595−3596.
(19) Collman, J. P.; Hutchison, J. E.; Ennis, M. S.; Lopez, M. A.; Guilard, R. *J. Am. Chem. Soc.* **1992**, *114*, 8074−8080.
(20) Collman, J. P.; Ha, Y.; Wagenknecht, P. S.; Lopez, M.-A.; Guilard, R. *J. Am. Chem. Soc.* **1993**, *115*, 9080−9088.
(21) Collman, J. P.; Wagenknecht, P. S.; Hutchison, J. E. *Angew. Chem., Int. Ed. Engl.* **1994**, *33*, 1537−1554.
(22) Naruta, Y.; Sasayama, M.; Sasaki, T. *Angew. Chem., Int. Ed. Engl.* **1994**, *33*, 1839−1841.
(23) Naruta, Y.; Sasayama, M. *J. Chem. Soc., Chem. Commun.* **1994**, 2667−2668.
(24) Collman, J. P.; Fish, H. T.; Wagenknecht, P. S.; Tyvoll, D. A.; Chng, L.-L.; Eberspacher, T. A.; Brauman, J. I.; Bacon, J. W.; Pignolet, L. H. *Inorg. Chem.* **1996**, *35*, 6746−6754.

10.1021/ic010871p CCC: $22.00
Published on Web 01/04/2002

(porphyrin) structural motif. These multiporphyrin compounds exploit a face-to-face bis(porphinato)metal core and auxiliary (porphinato)metal units that are linked to this structure via an ethyne-based macrocycle-to-macrocycle linkage topology, a mode of porphyrin-to-porphyrin connectivity that enables exceptional ground- and excited-state electronic communication between porphyrin centers.[25−32] Such oligo[(porphinato)metal] structures, featuring extensive porphyrin−porphyrin frontier orbital interactions enabled by both π-stacking and the cylindrically π-symmetric ethyne moiety, define potentially attractive ligand platforms from which to evolve new multielectron redox systems.

The fabrication of these species takes advantage of a new synthesis of 1,2-phenylene-bridged cofacial porphyrins[33] that exploits ethyne-bridged multiporphyrin precursors constructed via sequential Pd-catalyzed cross-coupling[25,34−40] and metal-templated [2+2+2] cycloaddition[41−44] reactions. In this study, we utilize this chemistry to synthesize face-to-face bis[(porphinato)metal] species that bear macrocycle−ethyne substituents; further application of Pd-catalyzed cross-coupling methodology extends conjugation of the cofacial (porphinato)metal core to additional porphyrin units, giving tris- and tetrakis[(porphinato)metal] compounds **1** and **2**, new multiporphyrin archetypes that feature macrocycle-to-macrocycle electronic communication that stems from both π-cofacial and π-conjugative interactions.

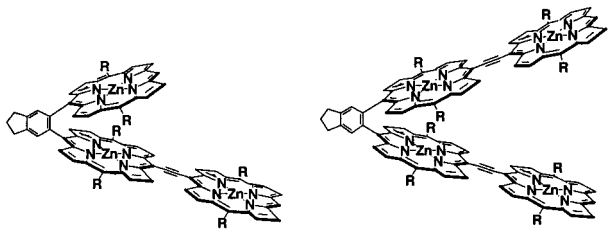

1 **2**

Experimental Section

All manipulations were carried out under nitrogen prepurified by passage through an O_2 scrubbing tower (Schweizerhall R3-11 catalyst) and a drying tower (Linde 3Å molecular sieves) unless otherwise stated. Air-sensitive solids were handled in a Braun 150-M glovebox. Standard Schlenk techniques were employed to manipulate air sensitive solutions. A syringe pump was utilized to control reproducibly the time-dependent concentration of reagents in these cycloaddition reactions.

Unless otherwise noted, all solvents utilized in this work were obtained from Fisher Scientific (HPLC grade); tetrahydrofuran and toluene were distilled from Na/benzophenone under N_2, and triethylamine was distilled from CaH_2 under N_2, while dioxane (anhydrous) was used as received from Aldrich. The catalysts Pd_2dba_3, $Pd(PPh_3)_2Cl_2$, $AsPh_3$, and $Co_2(CO)_8$ (Strem), as well as the reagents 1,6-heptadiyne, TBAF, iodobenzene, ethynylbenzene, CuI (Aldrich), trimethylacetylene, and triisopropylacetylene (GFS Chemicals) were used as received.

(5-Bromo-10,20-di[4-(3-methoxy-3-methylbutoxy)phenyl]porphinato)zinc(II), (5-ethynyl-10,20-di[4-(3-methoxy-3-methylbutoxy)-phenyl]porphinato)zinc(II), and (5,15-dibromo-10,20-di[4-(3-methoxy-3-methylbutoxy)phenyl]porphinato)zinc(II) were synthesized by methodology established previously.[25,40] Syntheses of spectroscopic benchmarks **12** and **13** are described in the Supporting Information.

Chromatographic purification (Silica 60, 230−400 mesh, EM Science, and Bio-Beads S-X1, 200−400 mesh, Bio-Rad) of all compounds was performed on the benchtop. Chemical shifts for ^{1}H NMR spectra are relative to residual protium in the deuterated solvents ($CDCl_3$, δ 7.24 ppm). All coupling constants are reported in Hertz.

Instrumentation. Electronic spectra were recorded on an OLIS UV−vis−NIR spectrophotometry system that is based on the optics of a Cary 14 spectrophotometer. NMR experiments were performed on a 250 MHz Brüker instrument. HRMS data were obtained at the Mass Spectral Laboratories of the Department of Chemistry, University of Pennsylvania. MALDI-TOF mass spectroscopic data were obtained with a Perseptive Voyager DE instrument in the Laboratories of Dr. Virgil Percec, Department of Chemistry, University of Pennsylvania. Samples were prepared as micromolar solutions in THF, and dithranol (Aldrich) was utilized as the matrix. Cyclic voltammetric experiments were performed with an EG&G Princeton Applied Research model 273A potentiostat/galvanostat. The cyclic voltammetric experiments utilized a single-compartment electrochemical cell with a platinum working electrode.

Bis[(5,5′-10,20-di[4-(3-methoxy-3-methylbutoxy)phenyl]porphinato)zinc(II)]ethyne (10). (5-Bromo-10,20-di[4-(3-methoxy-3-methylbutoxy)phenyl]porphinato)zinc(II) (53 mg, 0.063 mmol), (5-ethynyl-10,20-di[4-(3-methoxy-3-methylbutoxy)phenyl]porphinato)zinc(II) (45 mg, 0.058 mmol), $Pd_2(dba)_3$ (9 mg, 0.0093 mmol), and $AsPh_3$ (23 mg, 0.074 mmol) were added to a 50 mL Schlenk tube under N_2. THF (10 mL) and triethylamine (2 mL) were added via syringe, giving a deep green solution which was stirred for 3 h at 35 °C. The resulting green-brown solution was evaporated and the residue purified via chromatography (silica gel, 1/1 hexanes/THF). The green-brown band was collected and the solvent evaporated. The recovered solid was purified further via size-exclusion chromatography (SX-1 biobeads, THF). The dark green band was isolated, giving desired product **10**. Isolated yield = 83

(25) Lin, V. S.-Y.; DiMagno, S. G.; Therien, M. J. *Science* **1994**, *264*, 1105−1111.
(26) Lin, V. S.-Y.; Therien, M. J. *Chem.−Eur. J.* **1995**, *1*, 645−651.
(27) Kumble, R.; Palese, S.; Lin, V. S.-Y.; Therien, M. J.; Hochstrasser, R. M. *J. Am. Chem. Soc.* **1998**, *120*, 11489−11498.
(28) Shediac, R.; Gray, M. H. B.; Uyeda, H. T.; Johnson, R. C.; Hupp, J. T.; Angiolillo, P. J.; Therien, M. J. *J. Am. Chem. Soc.* **2000**, *122*, 7017−7033.
(29) Andersen, H. L. *Inorg. Chem.* **1994**, *33*, 972−981.
(30) Anderson, H. L. *Chem. Commun.* **1999**, 2323−2330.
(31) Arnold, D. P.; Heath, G. A.; James, D. A. *J. Porphyrins Phthalocyanines* **1999**, *3*, 5−31.
(32) Arnold, D. P. *Synlett* **2000**, 296−305.
(33) Fletcher, J. T.; Therien, M. J. *J. Am. Chem. Soc.* **2000**, *122*, 12393−12394.
(34) Heck, R. F. *Acc. Chem. Res.* **1979**, *12*, 146−151.
(35) Takahashi, S.; Kuroyama, Y.; Sonogashira, N.; Hagihara, N. *Synthesis* **1980**, 627−630.
(36) Kumada, M. *Pure Appl. Chem.* **1980**, *52*, 669−678.
(37) Negishi, E.-I.; Luo, F. T.; Frisbee, R.; Matsushita, H. *Heterocycles* **1982**, *18*, 117−122.
(38) Stille, J. K. *Angew. Chem., Int. Ed. Engl.* **1986**, *25*, 508−524.
(39) DiMagno, S. G.; Lin, V. S.-Y.; Therien, M. J. *J. Am. Chem. Soc.* **1993**, *115*, 2513−2515.
(40) DiMagno, S. G.; Lin, V. S.-Y.; Therien, M. J. *J. Org. Chem.* **1993**, *58*, 5983−5993.
(41) Vollhardt, K. P. C. *Angew. Chem., Int. Ed. Engl.* **1984**, *23*, 539−644.
(42) Schore, N. E. *Chem. Rev.* **1988**, *88*, 1081−1119.
(43) Chiusoli, G. P.; Costa, M.; Zhou, Z. *Gazz. Chim. Ital.* **1992**, *122*, 441−449.
(44) Lautens, M.; Klute, W.; Tam, W. *Chem. Rev.* **1996**, *96*, 49−92.

mg (93% based on 45 mg of the porphyrin starting material). ^{1}H NMR (250 MHz, 50/1 $CDCl_3$/d_5-pyridine): δ 10.45 (d, J = 4.53 Hz, 4H, β), 10.04 (s, 2H, *meso*), 9.24 (d, J = 4.43 Hz, 4H, β), 9.15 (d, J = 4.43 Hz, 4H, β), 8.98 (d, J = 4.35 Hz, 4H, β), 8.16 (d, J = 8.43 Hz, 8H, Ph), 7.31 (d, J = 8.53 Hz, 8H, Ph), 4.38 (t, J = 7.26 Hz, 8H, CH_2), 3.33 (s, 12H, OCH_3), 2.22 (t, J = 6.98 Hz, 8H, CH_2), 1.37 (s, 24H, CH_3). Vis (THF): 403 (5.08), 411 (5.08), 430 (5.00), 478 (5.46), 548 (4.21), 565 (4.18), 701 (4.69). MS (MALDI-TOF) *m*/*z*: 1535 (calcd for $C_{90}H_{86}N_8O_8Zn_2$ 1535).

5,6-Bis[(5,5′-10,20-di[4-(3-methoxy-3-methylbutoxy)phenyl]-porphinato)zinc(II)]indane (11). A 50 mL Schlenk tube was charged with **10** (50 mg, 33 μmol), $Co_2(CO)_8$ (11 mg, 33 μmol), dioxane (2.5 mL), and toluene (10 mL) under N_2. The resulting green solution was heated to 100 °C, following which 10 mL of a toluene solution containing 1,6-heptadiyne (38 μL, 330 μmol) and $Co_2(CO)_8$ (11 mg, 33 μmol) were added dropwise over an 18 h period. After the addition was complete, the solution was evaporated and the residue purified by chromatography (3/2 hexanes/THF). The red band was isolated, giving desired product **11**. Isolated yield = 50 mg (93% based on 50 mg of the porphyrin starting material). ^{1}H NMR (250 MHz, d_5-pyridine): δ 10.31 (d, J = 4.65 Hz, 4H, β), 10.11 (s, 2H, *meso*), 9.29 (d, J = 4.50 Hz, 4H, β), 9.13 (d, J = 4.68 Hz, 4H, β), 8.95 (d, J = 4.48 Hz, 4H, β), 8.64 (s, 2H, In CH), 8.02 (d, J = 8.28 Hz, 4H, Ph), 7.66 (d, J = 8.25 Hz, 4H, Ph), 7.32 (d, J = 8.33 Hz, 4H, Ph), 7.25 (d, J = 8.45 Hz, 4H, Ph), 4.43 (t, J = 7.06 Hz, 8H, R CH_2), 3.41 (t, J = 6.88 Hz, 4H, In CH_2), 3.30 (s, 12H, OCH_3), 2.40 (m, 2H, In CH_2), 2.26 (t, J = 6.98 Hz, 8H, R CH_2), 1.36 (s, 24H, CH_3). Vis (THF): 411 (5.54), 434 (4.74), 558 (4.32), 589 (3.72), 599 (3.71). MS (MALDI-TOF) *m*/*z*: 1627 (calcd for $C_{97}H_{94}N_8O_8Zn_2$ 1627).

(5-Ethynyl-15-triisopropylsilylethynyl-10,20-di[4-(3-methoxy-3-methylbutoxy)phenyl]porphinato)zinc(II) (5). (5,15-Dibromo-10,20-di[4-(3-methoxy-3-methylbutoxy)phenyl]porphinato)zinc-(II) (300 mg, 0.327 mmol), triisopropylsilylacetylene (0.47 mL, 2.094 mmol), trimethylsilylacetylene (0.10 mL, 0.698 mmol), Pd-$(PPh_3)_2Cl_2$ (24 mg, 0.035 mmol), and CuI (7 mg, 0.035 mmol) were added to a 50 mL Schlenk tube under N_2. THF (10 mL) and triethylamine (3 mL) were transferred to the Schlenk tube via syringe; the resulting deep green solution was stirred for 24 h at 45 °C. Over the course of the reaction, the solution became increasingly fluorescent when exposed to long wavelength UV irradiation from a hand-held lamp. After evaporation of volatiles, the residue was purified via chromatography (silica gel, 3/1 hexanes/THF). The dark green band was collected, which contained a mixture of three porphyrinic products. This mixture was dissolved in 50 mL of 1/1 THF/methanol, following which 1 M aqueous NaOH (2 mL) was added. After stirring 5 min at room temperature, the reaction was partitioned between CH_2Cl_2 and water, and the organic layer evaporated. The resulting mixture was purified via chromatography (silica gel, 7/3 hexanes/THF). The second dark green band isolated corresponded to the desired product **5**. Isolated yield = 138 mg (44% based on 300 mg of the porphyrin starting material). ^{1}H NMR (250 MHz, 50/1 $CDCl_3$/d_5-pyridine): δ 9.65 (d, J = 4.55 Hz, 2H, β), 9.60 (d, J = 4.57 Hz, 2H, β), 8.86 (d, J = 4.56 Hz, 2H, β), 8.85 (d, J = 4.56 Hz, 2H, β), 8.02 (d, J = 8.57 Hz, 4H, Ph), 7.24 (d, J = 8.58 Hz, 4H, Ph), 4.34 (t, J = 7.16 Hz, 4H, CH_2), 4.10 (s, 1H, CCH), 3.32 (s, 6H, OCH_3), 2.20 (t, J = 7.13 Hz, 4H, CH_2), 1.39 (s, 21H, TIPS), 1.35 (s, 12H, CH_3). Vis (THF): 434 (5.50), 446 (5.35), 538 (3.48), 582 (4.06), 632 (4.46). HRMS (ESI+) *m*/*z*: 960.396104 (calcd for $C_{57}H_{64}N_4O_4SiZn$ 960.398831). The first dark green band isolated corresponded to the (5,15-bis[triisoproplysilylethynyl]-10,20-di[4-(3-methoxy-3-methylbutoxy)phenyl]porphinato)zinc(II) side product. Isolated yield = 49 mg (13% based on 300 mg of the porphyrin starting material). ^{1}H NMR (250 MHz, 50/1 $CDCl_3$/d_5-pyridine): δ 9.63 (d, J = 4.50 Hz, 4H, β), 8.84 (d, J = 4.44 Hz, 4H, β), 8.01 (d, J = 8.59 Hz, 4H, Ph), 7.22 (d, J = 8.59 Hz, 4H, Ph), 4.34 (t, J = 7.27 Hz, 4H, CH_2), 3.32 (s, 6H, OCH_3), 2.20 (t, J = 6.97 Hz, 4H, CH_2), 1.39 (s, 42H, TIPS), 1.35 (s, 12H, CH_3). The third dark green band isolated corresponded to the (5,15-diethynyl-10,20-di[4-(3-methoxy-3-methylbutoxy)phenyl]porphinato)zinc(II) side product. Isolated yield = 110 mg (42% based on 300 mg of the porphyrin starting material). ^{1}H NMR (250 MHz, 50/1 $CDCl_3$/d_5-pyridine): δ 9.62 (d, J = 4.62 Hz, 4H, β), 8.86 (d, J = 4.65 Hz, 4H, β), 8.02 (d, J = 8.60 Hz, 4H, Ph), 7.24 (d, J = 8.59 Hz, 4H, Ph), 4.34 (t, J = 7.15 Hz, 4H, CH_2), 4.11 (s, 2H, CCH), 3.31 (s, 6H, OCH_3), 2.20 (t, J = 7.15 Hz, 4H, CH_2), 1.35 (s, 12H, CH_3).

(5-Triisoproplysilylethynyl-15,15′-bis[(10,20-di[4-(3-methoxy-3-methylbutoxy)phenyl]porphinato)zinc(II)])ethyne (6). (5-Bromo-10,20-di[4-(3-methoxy-3-methylbutoxy)phenyl]porphinato)-zinc(II) (107 mg, 0.128 mmol), **5** (113 mg, 0.118 mmol), $Pd_2(dba)_3$ (17 mg, 0.019 mmol), and $AsPh_3$ (46 mg, 0.15 mmol) were added to a 100 mL Schlenk tube under N_2. THF (15 mL) and triethylamine (3 mL) were added via syringe, giving a green solution which was stirred for 4 h at 40 °C. Following evaporation of volatiles, the residue was purified via chromatography (silica gel, 1/1 hexanes/THF). A dark green-brown band was collected, which was purified further via size-exclusion chromatography (SX-1 biobeads, THF), giving desired product **6**. Isolated yield = 0.186 g (92% based on 113 mg of starting material **5**). ^{1}H NMR (250 MHz, 50/1 $CDCl_3$/d_5-pyridine): δ 10.40 (d, J = 4.60 Hz, 2H, β), 10.34 (d, J = 4.55 Hz, 2H, β), 10.03 (s, 1H, *meso*), 9.65 (d, J = 4.58 Hz, 2H, β), 9.22 (d, J = 4.50 Hz, 2H, β), 9.13 (d, J = 4.58 Hz, 2H, β), 9.02 (d, J = 4.53 Hz, 2H, β), 8.96 (d, J = 4.45 Hz, 2H, β), 8.88 (d, J = 4.53 Hz, 2H, β), 8.14 (d, J = 8.63 Hz, 4H, Ph), 8.09 (d, J = 8.70 Hz, 4H, Ph), 7.29 (d, J = 8.50 Hz, 4H, Ph), 7.26 (d, J = 8.58 Hz, 4H, Ph), 4.37 (t, J = 7.12 Hz, 4H, CH_2), 4.36 (t, J = 7.12 Hz, 4H, CH_2), 3.31 (s, 12H, OCH_3), 2.20 (t, J = 7.12 Hz, 8H, CH_2), 1.40 (m, 21H, TIPS), 1.35 (s, 24H, CH_3). Vis (THF): 412 (5.13), 423 (5.13), 448 (5.01), 482 (5.48), 558 (4.26), 727 (4.84). MS (MALDI-TOF) *m*/*z*: 1715 (calcd for $C_{101}H_{106}N_8O_8SiZn_2$ 1714).

5-[(5′-15′-Triisopropylsilylethynyl-10′,20′-di[4-(3-methoxy-3-methylbutoxy)phenyl]porphinato)zinc(II)]-6-[(5″-10″,20″-di-[4-(3-methoxy-3-methylbutoxy)phenyl]porphinato)zinc-(II)]indane (8). A 50 mL Schlenk tube was charged with **6** (80 mg, 47 μmol), $Co_2(CO)_8$ (25 mg, 71 μmol), dioxane (2.5 mL), and toluene (10 mL). The resulting green solution was heated to 100 °C, following which 5 mL of a toluene solution containing 1,6-heptadiyne (54 μL, 470 μmol) were added dropwise over a 17 h period. After the addition was complete, the solution was evaporated and the residue purified by chromatography (silica gel, 7/3 hexanes/THF). The purple-green band was isolated giving the desired product **8**. Isolated yield = 58 mg (68% based on 80 mg of the porphyrin starting material). ^{1}H NMR (250 MHz, 50/1 $CDCl_3$/d_5-pyridine): δ 9.73 (s, 1H, meso), 9.65 (d, J = 4.67 Hz, 2H, β), 9.60 (d, J = 4.69 Hz, 2H, β), 9.38 (d, J = 4.43 Hz, 2H, β), 8.97 (d, J = 4.57 Hz, 2H, β), 8.66 (d, J = 4.42 Hz, 2H, β), 8.63 (d, J = 4.40 Hz, 2H, β), 8.55 (d, J = 4.51 Hz, 2H, β), 8.49 (d, J = 4.68 Hz, 2H, β), 8.33 (s, 1H, In CH), 8.30 (s, 1H, In CH), 7.75 (m, 4H, Ph), 7.50 (m, 4H, Ph), 7.11 (m, 8H, Ph), 4.31 (t, J = 7.04 Hz, 4H, R CH_2), 4.30 (t, J = 6.88 Hz, 4H, R CH_2), 3.43 (t, J = 6.99 Hz, 4H, In CH_2), 3.31 (s, 12H, OCH_3), 2.55 (m, 2H, In CH_2), 2.19 (t, J = 7.11 Hz, 4H, R CH_2), 2.17 (t, J = 7.11 Hz, 4H, R CH_2), 1.35 (s, 24H, CH_3), 1.27 (s, 21H, TIPS). Vis (THF): 416 (5.60), 443 (5.04), 557 (4.30), 572 (4.28), 623 (4.28). MS (MALDI-TOF) *m*/*z*: 1806 (calcd for $C_{108}H_{114}N_8O_8SiZn_2$ 1807). A trailing brown

band was also isolated, which corresponded to pure starting material **6**. Isolated yield = 26 mg (32% recovery based on 80 mg of the porphyrin starting material).

5-[(5′-15′-Ethynyl-10′,20′-di[4-(3-methoxy-3-methylbutoxy)-phenyl]porphinato)zinc(II)]-6-[(5″-10″,20″-di[4-(3-methoxy-3-methylbutoxy)phenyl]porphinato)zinc(II)]indane (3). A 50 mL Schlenk tube was charged with **8** (58 mg, 0.032 mmol), THF (5 mL), and tetrabutylammonium fluoride (1.0 M in THF, 0.068 mL, 0.068 mmol). After stirring 10 min at room temperature, $CHCl_3$ (100 mL) was added to the reaction. The resulting solution was washed with $NaHCO_3$ (aq), following which the organic layer was separated, evaporated, and purified via chromatography (silica gel, 3/2 hexanes/THF). The purple-brown band was isolated, giving the desired product **3**. Isolated yield = 44 mg (83% based on 58 mg of the porphyrin starting material). ^{1}H NMR (250 MHz, 50/1 $CDCl_3$/d_5-pyridine): δ 9.74 (s, 1H, meso), 9.65 (d, J = 4.65 Hz, 2H, β), 9.62 (d, J = 4.62 Hz, 2H, β), 9.35 (d, J = 4.68 Hz, 2H, β), 8.98 (d, J = 4.48 Hz, 2H, β), 8.66 (d, J = 4.46 Hz, 2H, β), 8.62 (d, J = 4.59 Hz, 2H, β), 8.56 (d, J = 4.64 Hz, 2H, β), 8.50 (d, J = 4.64 Hz, 2H, β), 8.34 (s, 1H, In CH), 8.32 (s, 1H, In CH), 7.76 (m, 4H, Ph), 7.50 (m, 4H, Ph), 7.12 (m, 8H, Ph), 4.32 (t, J = 7.12 Hz, 8H, R CH_2), 3.91 (s, 1H, CCH), 4.31 (t, J = 7.16 Hz, 8H, R CH_2), 3.45 (t, J = 7.16 Hz, 4H, In CH_2), 3.32 (s, 12H, OCH_3), 2.56 (m, 2H, In CH_2), 2.19 (t, J = 7.12 Hz, 8H, R CH_2), 1.37 (s, 24H, CH_3). Vis (THF): 416 (5.60), 443 (5.04), 557 (4.30), 572 (4.28), 623 (4.28). MS (MALDI-TOF) m/z: 1651 (calcd for $C_{99}H_{94}N_8O_8Zn_2$ 1651).

5-(5′-[15′,15″-Bis(10″,20″-di[4-(3-methoxy-3-methylbutoxy)-phenyl]porphinato)zinc(II)]ethyne)-6-[(5‴-10‴,20‴-di[4-(3-methoxy-3-methylbutoxy)phenyl]porphinato)zinc(II)]indane (1). (5-Bromo-10,20-di[4-(3-methoxy-3-methylbutoxy)phenyl]porphinato)zinc(II) (17 mg, 0.0203 mmol), **3** (28 mg, 0.0170 mmol), $Pd_2(dba)_3$ (3 mg, 0.0033 mmol), and $AsPh_3$ (8 mg, 0.0262 mmol) were added to a 50 mL Schlenk tube under N_2. THF (5 mL) and triethylamine (1 mL) were added via syringe, and the reaction was stirred for 16 h at 45 °C. Following evaporation of volatiles, the residue was purified via chromatography (silica gel, 3/2 hexanes/THF). The brown band was isolated giving desired product **1**. Isolated yield = 32 mg (78% based on 28 mg of starting material **3**). ^{1}H NMR (250 MHz, 50/1 $CDCl_3$/d_5-pyridine): δ 10.27 (d, J = 4.55 Hz, 2H, β), 10.10 (d, J = 4.50 Hz, 2H, β), 9.99 (s, 1H, meso), 9.74 (s, 1H, meso), 9.70 (d, J = 4.68 Hz, 2H, β), 9.63 (d, J = 4.70 Hz, 2H, β), 9.19 (d, J = 4.43 Hz, 2H, β), 9.03 (d, J = 4.55 Hz, 2H, β), 8.99 (d, J = 4.40 Hz, 2H, β), 8.92 (d, J = 4.33 Hz, 2H, β), 8.74 (d, J = 4.58 Hz, 2H, β), 8.68 (d, J = 4.43 Hz, 2H, β), 8.66 (d, J = 4.65 Hz, 2H, β), 8.54 (d, J = 4.65 Hz, 2H, β), 8.36 (s, 1H, In CH), 8.35 (s, 1H, In CH), 8.08 (d, J = 8.28 Hz, 4H, Ph), 7.81 (m, 4H, Ph), 7.57 (m, 4H, Ph), 7.25 (d, J = 7.40 Hz, 4H, Ph), 7.14 (m, 8H, Ph), 4.34 (t, J = 7.04 Hz, 4H, R CH_2), 4.33 (t, J = 7.09 Hz, 4H, R CH_2), 4.32 (t, J = 7.05 Hz, 4H, R CH_2), 3.46 (m, 4H, In CH_2), 3.33 (s, 6H, OCH_3), 3.32 (s, 6H, OCH_3), 3.31 (s, 6H, OCH_3), 2.57 (m, 2H, In CH_2), 2.20 (t, J = 7.03 Hz, 4H, R CH_2), 2.19 (t, J = 7.00 Hz, 8H, R CH_2), 1.38 (s, 12H, CH_3), 1.37 (s, 12H, CH_3), 1.35 (s, 12H, CH_3). Vis (THF): 411 (5.44), 487 (5.27), 557 (4.41), 714 (4.70). MS (MALDI-TOF) m/z: 2406 (calcd for $C_{143}H_{138}N_{12}O_{12}Zn_3$ 2407).

Bis[(5,5′-15-triisopropylsilylethynyl-10,20-di[4-(3-methoxy-3-methylbutoxy)phenyl]porphinato)zinc(II)]ethyne (7). A 50 mL Schlenk tube was charged with **14** (0.152 g, 0.150 mmol), **5** (0.130 mg, 0.135 mmol), $Pd_2(dba)_3$ (0.020 g, 0.022 mmol), $AsPh_3$ (0.053 g, 0.172 mmol), THF (15 mL), and triethylamine (3 mL), giving a deep green solution, which was stirred for 4 h at 40 °C. Following evaporation of the solvent, the residue was purified via chromatography (silica gel, 3/2 hexanes/THF). The green-brown band was isolated, giving desired product **7**. Isolated yield = 0.235 g (92% based on 0.130 g of starting material **5**). ^{1}H NMR (250 MHz, 50/1 $CDCl_3$/d_5-pyridine): δ 10.29 (d, J = 4.53 Hz, 4H, β), 9.65 (d, J = 4.60 Hz, 4H, β), 9.01 (d, J = 4.55 Hz, 4H, β), 8.85 (d, J = 4.58 Hz, 4H, β), 8.09 (d, J = 8.43 Hz, 8H, Ph), 7.27 (d, J = 8.63 Hz, 8H, Ph), 4.36 (t, J = 7.09 Hz, 8H, CH_2), 3.32 (s, 12H, OCH_3), 2.20 (t, J = 7.13 Hz, 8H, CH_2), 1.39 (m, 42H, TIPS), 1.36 (s, 24H, CH_3). Vis (THF): 424 (5.22), 436 (5.20), 488 (5.47), 576 (4.25), 747 (4.91). MS (MALDI-TOF) m/z: 1895 (calcd for $C_{112}H_{126}N_8O_8Si_2Zn_2$ 1895).

5,6-Bis[(5′-15′-triisopropylsilylethynyl-10′,20′-di[4-(3-methoxy-3-methylbutoxy)phenyl]porphinato)zinc(II)]indane (9). A 50 mL Schlenk tube was charged with **7** (65 mg, 34.3 μmol), $Co_2(CO)_8$ (18 mg, 51.5 μmol), dioxane (2.5 mL), and toluene (10 mL). The resulting brown solution was heated to 100 °C, following which 5 mL of a toluene solution containing 1,6-heptadiyne (40 μL, 343 μmol) were added dropwise over a 17 h period. After the addition was complete, the resulting green solution was evaporated and the residue purified by chromatography (silica gel, 7/3 hexanes/THF). The green band was isolated giving the desired product **9**. Isolated yield = 50 mg (73% based on 65 mg of the porphyrin starting material). ^{1}H NMR (250 MHz, 50/1 $CDCl_3$/d_5-pyridine): δ 9.56 (d, J = 4.71 Hz, 4H, β), 9.40 (d, J = 4.45 Hz, 4H, β), 8.57 (d, J = 4.44 Hz, 4H, β), 8.50 (d, J = 4.70 Hz, 4H, β), 8.29 (s, 2H, In CH), 7.75 (m, 4H, Ph), 7.48 (m, 4H, Ph), 7.11 (m, 8H, Ph), 4.31 (t, J = 7.13 Hz, 8H, R CH_2), 3.44 (t, J = 7.00 Hz, 4H, In CH_2), 3.30 (s, 12H, OCH_3), 2.55 (m, 2H, In CH_2), 2.20 (t, J = 7.08 Hz, 8H, R CH_2), 1.37 (s, 24H, CH_3), 1.23 (m, 42H, TIPS). Vis (THF): 423 (5.43), 428 (5.43), 454 (4.87), 577 (4.29), 613 (4.22), 625 (4.32). MS (MALDI-TOF) m/z: 1986 (calcd for $C_{119}H_{134}N_8O_8Si_2Zn_2$ 1987). A trailing brown band was also isolated, which corresponded to pure porphyrinic starting material. Isolated yield = 17 mg (26% recovery based on 65 mg of compound **7**).

5,6-Bis[(5′,5″-15′-ethynyl-10′,20′-di[4-(3-methoxy-3-methylbutoxy)phenyl]porphinato)zinc(II)]indane (4). A 50 mL Schlenk tube was charged with **9** (58 mg, 0.029 mmol), THF (5 mL), and tetrabutylammonium fluoride (1.0 M in THF, 0.09 mL, 0.09 mmol). After stirring 10 min at room temperature, $CHCl_3$ (100 mL) was added, and the resulting solution was washed with $NaHCO_3$ (aq). The organic layer was separated, evaporated, and purified via chromatography (silica gel, 7/3 hexanes/THF). The green band was isolated, giving desired product **4**. Isolated yield = 47 mg (98% based on 58 mg of the porphyrin starting material). ^{1}H NMR (250 MHz, 50/1 $CDCl_3$/d_5-pyridine): δ 9.56 (d, J = 4.52 Hz, 4H, β), 9.36 (d, J = 4.61 Hz, 4H, β), 8.57 (d, J = 4.63 Hz, 4H, β), 8.50 (d, J = 4.66 Hz, 4H, β), 8.30 (s, 2H, In CH), 7.73 (m, 4H, Ph), 7.47 (m, 4H, Ph), 7.11 (m, 8H, Ph), 4.31 (t, J = 7.12 Hz, 8H, R CH_2), 3.92 (s, 2H, CCH), 3.44 (t, J = 7.14 Hz, 4H, In CH_2), 3.32 (s, 12H, OCH_3), 2.55 (m, 2H, In CH_2), 2.19 (t, J = 7.12 Hz, 8H, R CH_2), 1.36 (s, 24H, CH_3). Vis (THF): 423 (5.43), 428 (5.43), 454 (4.87), 577 (4.29), 613 (4.22), 625 (4.32). MS (MALDI-TOF) m/z: 1671 (calcd for $C_{101}H_{94}N_8O_8Zn_2$ 1675).

5,6-Bis(5′-15′,15″-bis[(10′,20′-di[4-(3-methoxy-3-methylbutoxy)phenyl]porphinato)zinc(II)]ethyne)indane (2). (5-Bromo-10,20-di[4-(3-methoxy-3-methylbutoxy)phenyl]porphinato)zinc-(II) (31 mg, 0.0370 mmol), **4** (30 mg, 0.0180 mmol), $Pd_2(dba)_3$ (5 mg, 0.0054 mmol), $AsPh_3$ (0.013 g, 0.043 mmol), THF (10 mL), and triethylamine (2 mL) were added to a 50 mL Schlenk tube. The resulting solution was stirred for 23 h at 40 °C. Following evaporation of volatiles, the residue was purified via chromatography (silica gel, 1/1 hexanes/THF). The brown band was collected and purified further via size-exclusion chromatography (SX-1

biobeads, THF), giving desired product **2**. Isolated yield = 36 mg (63% based on 30 mg of starting material **4**). ^{1}H NMR (250 MHz, 50/1 $CDCl_3/d_5$-pyridine): δ 10.27 (d, J = 4.55 Hz, 4H, β), 10.13 (d, J = 4.63 Hz, 4H, β), 9.98 (s, 2H, *meso*), 9.63 (d, J = 4.70 Hz, 4H, β), 9.18 (d, J = 4.45 Hz, 4H, β), 9.02 (d, J = 4.50 Hz, 4H, β), 8.91 (d, J = 4.45 Hz, 4H, β), 8.78 (d, J = 4.50 Hz, 4H, β), 8.59 (d, J = 4.58 Hz, 4H, β), 8.36 (s, 2H, In CH), 8.07 (d, J = 8.43 Hz, 8H, Ph), 7.86 (m, 4H, Ph), 7.63 (m, 4H, Ph), 7.20 (m, 16H, Ph), 4.35 (t, J = 7.13 Hz, 8H, R CH_2), 4.32 (t, J = 7.13 Hz, 8H, R CH_2), 3.48 (t, J = 7.03 Hz, 4H, In CH_2), 3.35 (s, 12H, OCH_3), 3.29 (s, 12H, OCH_3), 2.58 (m, 2H, In CH_2), 2.22 (t, J = 7.13 Hz, 8H, R CH_2), 2.19 (t, J = 7.13 Hz, 8H, R CH_2), 1.40 (s, 24H, CH_3), 1.33 (s, 24H, CH_3). Vis (THF): 419 (5.39), 479 (5.35), 558 (4.51), 713 (4.85). MS (MALDI-TOF) *m/z*: 3182 (calcd for $C_{189}H_{178}N_{16}O_{16}Zn_4$ 3183).

X-ray Crystallographic Structural Determination of 5,6-Bis[(5′-15′-triisopropylsilylethynyl-10′,20′-di[4-(3-methoxy-3-methylbutoxy)phenyl]porphinato)zinc(II)]indane)·(Ethanol)$_2$ (9·(EtOH)$_2$). X-ray quality crystals of **9·(EtOH)$_2$** were obtained from slow diffusion of ethanol into a chloroform solution of **9**. The crystal dimensions were 0.30 × 0.25 × 0.20 mm^3. Compound **9·(EtOH)$_2$** crystallizes in the triclinic space group $P\bar{1}$ with a = 19.5111(7) Å, b = 20.9667(6) Å, c = 17.5249(6) Å, α = 103.699(2)°, β = 110.344(2)°, γ = 86.690(3)°, V = 6528.3(4) Å^3, Z = 2, and d_{calcd} = 1.060 g/cm^3. X-ray intensity data were collected on a Rigaku R-AXIS IIc area detector employing graphite-monochromated Mo Kα radiation (λ = 0.710 69 Å) at a temperature of 200 K. Indexing was performed from a series of 1° oscillation images with exposures of 200 s per frame. A hemisphere of data was collected using 4° oscillation angles with exposures of 1200 s per frame and a crystal-to-detector distance of 82 mm. Oscillation images were processed using bioteX,[45] producing a listing of unaveraged F^2 and $\sigma(F^2)$ values which were then passed to the teXsan[46] program package for further processing and structure solution on a Silicon Graphics Indigo R4000 computer. A total of 46 248 reflections were measured over the ranges $5.02 \le 2\theta \le 50.7°$, $-23 \le h \le 23$, $-25 \le k \le 25$, $-21 \le l \le 21$ yielding 20 964 unique reflections (R_{int} = 0.0632). The intensity data were corrected for Lorentz and polarization effects but not for absorption.

The structure of **9·(EtOH)$_2$** was solved by Patterson methods (DIRDIF).[47] Table 1 contains details of the crystal and data collection parameters. The structure was determined by Dr. Patrick Carroll at the X-ray facility at the Department of Chemistry, University of Pennsylvania.

Refinement was by full-matrix least squares based on F^2 using SHELXL-93.[48] All reflections were used during refinement (F^2 values that were experimentally negative were replaced by F^2 = 0). The weighting scheme used was $w = 1/[\sigma^2(F_o^2) + 0.1010P^2 + 22.8370P]$ where $P = (F_o^2 + 2F_c^2)/3$. Non-hydrogen atoms were refined anisotropically, and hydrogen atoms were refined using a "riding" model. Refinement converged to R1 = 0.1041 and wR2 = 0.2366 for 15 783 reflections for which $F > 4\sigma(F)$, and R1 = 0.1321, wR2 = 0.2533, and GOF = 1.160 for all 20 964 unique, nonzero reflections and 1324 variables.[49] The maximum Δ/σ in the final cycle of least squares was −0.003, and the two most prominent peaks in the final difference Fourier were +0.713 and −0.381 e/Å^3.

Table 1. Summary of Structure Determination of 5,6-Bis[(5′-15′-triisopropylsilylethynyl-10′,20′-di[4-(3-methoxy-3-methylbutoxy)-phenyl]porphinato)zinc(II)]indane)·(Ethanol)$_2$ (**9·(EtOH)$_2$**)

formula	$Zn_2C_{123}H_{146}Si_2N_8O_{10}$
fw	2083.40
cryst class	triclinic
space group	$P\bar{1}$ (No. 2)
Z	2
cell constants	
a	19.5111(7) Å
b	20.9667(6) Å
c	17.5249(6) Å
*h*ind;1*g*α	103.699(2)°
b	110.344(2)°
hind;1gγ	86.690(3)°
V	6528.3(4) Å^3
μ	4.39 cm^{-1}
crystal size, mm^3	0.30 × 0.25 × 0.20
D_{calcd}	1.060 g/cm^3
F(000)	2216
radiation	Mo Kα (λ = 0.710 69 Å)
2θ range	5.02−50.7°
hkl collected	$-23 \le h \le 23$; $-25 \le k \le 25$; $-21 \le l \le 21$
no. reflns measured	46 248
no. unique reflns	20 964 (R_{int} = 0.0632)
no. obsd reflns	15 783 ($F > 4\sigma$)
no. reflns used in refinement	20 964
no. params	1324
R indices ($F > 4\sigma$)	R1 = 0.1041 wR2 = 0.2366
R indices (all data)	R1 = 0.1321 wR2 = 0.2533
GOF	1.160
final difference peaks, e/Å^3	+0.713, −0.381

Scheme 1

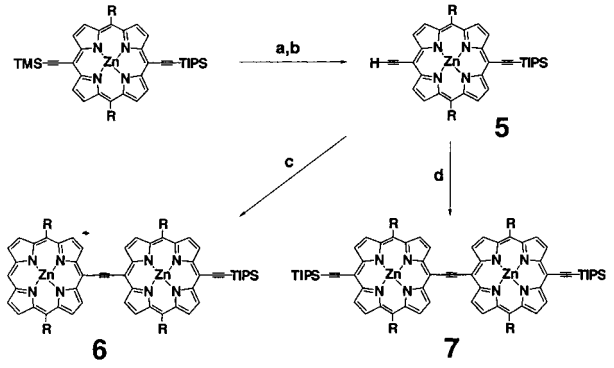

[a] Trimethylsilylacetylene (2 equiv), triisopropylsilylacetylene (6 equiv), $Pd(PPh_3)_2Cl_2$ (10 mol %), CuI (10 mol %), THF/TEA 10/3, 45 °C, 24 h. [b] 1.0 M NaOH (1 equiv), THF/MeOH 1/1, 25 °C, 10 min (**5**, 44%). [c] (5-Bromo-10,20-di[4-(3-methoxy-3-methylbutoxy)phenyl]porphinato)zinc(II) (1.1 equiv), Pd_2dba_3 (15 mol %), $AsPh_3$ (1.2 equiv), THF/TEA 5/1, 40 °C, 4 h (**6**, 93%). [d] (5-Bromo-15-triisopropylsilylethynyl-10,20-di[4-(3-methoxy-3-methylbutoxy)phenyl]porphinato)zinc(II) (1.1 equiv), Pd_2dba_3 (15 mol %), $AsPh_3$ (1.2 equiv), THF/TEA 5/1, 40 °C, 4 h (**7**, 92%).

Results and Discussion

Synthesis. Scheme 1 outlines the syntheses of (5-triisopropylsilylethynyl-15,15′-bis[(10,20-di[4-(3-methoxy-3-methylbutoxy)phenyl]porphinato)zinc(II)])ethyne (**6**) and bis-[(5,5′-15-triisopropylsilylethynyl-10,20-di[4-(3-methoxy-3-

(45) *bioteX*: *A suite of Programs for the Collection, Reduction and Interpretation of Imaging Plate Data*; Molecular Structure Corporation: The Woodlands, TX, 1995.
(46) *teXsan*: *Crystal Structure Analysis Package*; Molecular Structure Corporation: The Woodlands, TX, 1985, 1992.
(47) *DIRDIF*: Parthasavathi, V.; Beurskens, P. T.; Slot, H. J. B. *Acta Crystallogr*. **1983,** *A39*, 860.
(48) Sheldrick, G. M. *SHELXL-93*: *Program for the Refinement of Crystal Structures*; University of Göttingen: Germany, 1993.
(49) $R1 = \sum||F_o| - |F_c||/\sum|F_o|$, $wR2 = \{\sum w(F_o^2 - F_c^2)^2/\sum w(F_o^2)^2\}^{1/2}$, $GOF = \{\sum w(F_o^2 - F_c^2)^2/\sum(n - p)\}^{1/2}$, where n = the number of reflections and p = the number of parameters refined.

Scheme 2

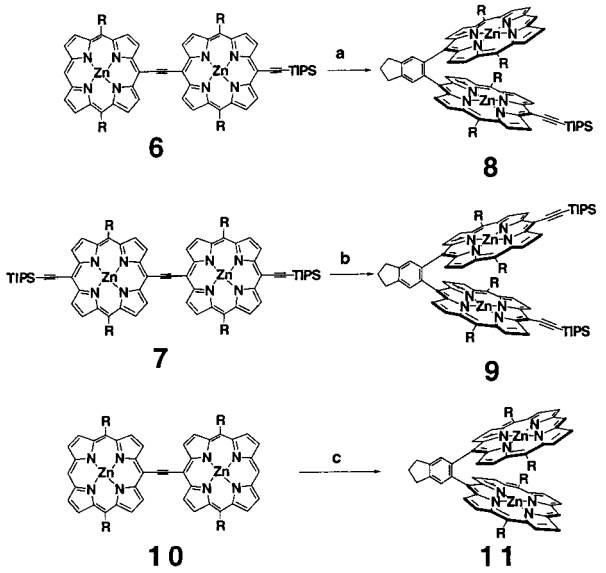

[a] 1,6-Heptadiyne (10 equiv), $Co_2(CO)_8$ (1.5 equiv), dioxane/toluene 4/1, 100 °C, 17 h (**8**, 68%). [b] 1,6-Heptadiyne (10 equiv), $Co_2(CO)_8$ (1.5 equiv), dioxane/toluene 4/1, 100 °C, 17 h (**9**, 73%). [c] 1,6-Heptadiyne (10 equiv), $Co_2(CO)_8$ (2 equiv), dioxane/toluene 4/1, 100 °C, 18 h (**11**, 94%).

methylbutoxy)phenyl]porphinato)zinc(II)]ethyne (**7**), key precursors to structures **1** and **2**. The synthetic strategy exploits the facts that cobalt-catalyzed [2+2+2] cycloaddition reactions are sensitive to alkyne steric properties,[41,50] and that [5-(trimethylsilylethynyl)-15-(triisopropylsilylethynyl)-10,-20-diarylporphinato]zinc(II) species can be prepared readily. Selective deprotection of the trimethylsilyl (TMS) group using standard methods[35,51] gives [5-ethynyl-15-(triisopropylsilylethynyl)-10,20-di[4-(3-methoxy-3-methylbutoxy)phenyl]porphinato]zinc(II) (**5**); reaction of TIPS-protected **5** with the corresponding 5-bromo- and 5-bromo-15-triisopropylsilylethynyl-substituted 10,20-diarayl(porphinato)zinc(II) compounds under previously established reaction conditions[25,52] gives **6** and **7**.

Meso-to-*meso* ethyne-bridged bis(porphinato)zinc(II) species **6** and **7** undergo [2+2+2] cycloadditions with 1,6-heptadiyne exclusively at the ethynyl moiety that links the two porphyryl macrocycles (Scheme 2) to yield cofacial bis-[(porphinato)zinc(II)] species **8** and **9**. These reactions occur in yields (~70%, based on the porphyrinic starting material) comparable to that delineated for the conversion of the simple conjugated dimeric (porphinato)zinc(II) species **10** to face-to-face **11**.[33]

Compounds **8** and **9** can be deprotected using tetra-*n*-butylammonium fluoride to yield **3** and **4**, respectively; subsequent Pd-catalyzed cross-coupling reactions of synthons **3** and **4** with [5-bromo-10,20-di[4-(3-methoxy-3-methylbutoxy)-phenyl]porphinato]zinc(II) complete the syntheses of supermolecular (porphinato)metal species **1** and **2** (Scheme 3).

Scheme 3

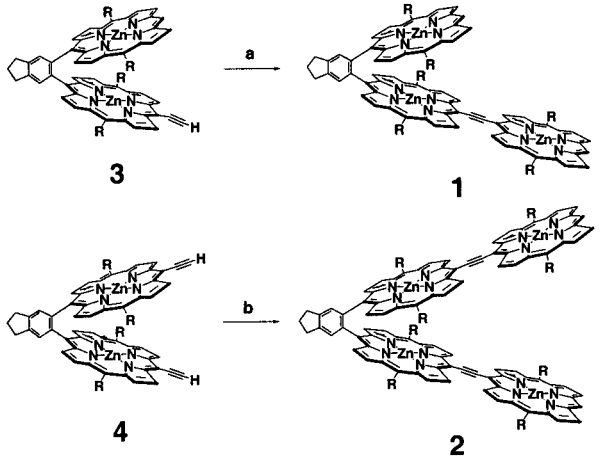

[a] (5-Bromo-10,20-di[4-(3-methoxy-3-methylbutoxy)phenyl]porphinato)zinc(II) (1.2 equiv), Pd_2dba_3 (18 mol %), $AsPh_3$ (1.4 equiv), THF/TEA 5/1, 45 °C, 5 h (**1**, 78%). [b] (5-Bromo-10,20-di[4-(3-methoxy-3-methylbutoxy)phenyl]porphinato)zinc(II) (2.2 equiv), Pd_2dba_3 (30 mol %), $AsPh_3$ (2.4 equiv), THF/TEA 5/1, 40 °C, 23 h (**2**, 65%).

Structural Studies. The ORTEP representation of 5,6-bis[(5′-15′-triisopropylsilylethynyl-10′,20′-di[4-(3-methoxy-3-methylbutoxy)phenyl]porphinato)zinc(II)]indane)·(ethanol)$_2$ (**9·(EtOH)$_2$**) is shown in Figure 1, with thermal ellipsoids displayed at 30% probability. This structurally characterized 1,2-phenylene-linked bis(porphyrin) species featuring a cavity-bound ethanol constitutes an additional example of the open "Pac-Man"[53] conformation.[33] Key metrical parameters for **9·(EtOH)$_2$** include a Zn−Zn distance of 6.92 Å, a substantial 64.5° dihedral angle between the least squares planes defined by the respective four central nitrogen atoms (N4 plane) of its (porphinato)zinc(II) units, and a lateral shift[54] between the two porphyryl Zn atoms of 4.16 Å.

Congruent with the open structure of **9·(EtOH)$_2$**, small amplitude bond length and bond angle distortions are evident at the juncture where the indanyl 5- and 6-carbon atoms are linked to the 5′-(porphinato)zinc(II) *meso* positions (Figures 1−2, Table 2). The indanyl C_6/C_5-to-*meso* carbon distances (C17−C58 and C66−C68) are elongated slightly (~0.02 Å) relative to typical C_{meso}-to-arene bonds. Likewise, the corresponding C17−C58−C66 and C68−C66−C58 bond angles (~123.2°) reflect the steric crowding at the 5,6-indanyl bridge that links the two (porphinato)metal units.

Each porphyrin macrocycle of **9·(EtOH)$_2$** exhibits a combination of ruffling and saddling distortions (Figure 2). The mean deviations of the macrocyclic carbon atoms from the N4 planes are 0.133 and 0.119 Å, respectively, for the Zn1 and Zn2 ring systems. For the Zn1 ring system, the typical C_{meso} and C_β displacements from the porphyrin least squares plane are respectively 0.184 and 0.114 Å, respectively, while the corresponding C_{meso} and C_β displacements within the Zn2 macrocycle are 0.146 and 0.121 Å. The closest nonbonded contact between each of the porphyrin

(50) Hillard, R. L., III; Vollhardt, K. P. C. *J. Am. Chem. Soc.* **1977**, *99*, 4058−4069.
(51) Zehner, R. W.; Parsons, B. F.; Hsung, R. P.; Sita, L. R. *Langmuir* **1999**, *15*, 1121−1127.
(52) Wagner, R. W.; Johnson, T. E.; Li, F.; Lindsey, J. S. *J. Org. Chem.* **1995**, *60*, 5266−5273.
(53) Guilard, R.; Brandes, S.; Tardieux, C.; Tabard, A.; L'Her, M.; Miry, C.; Gouerec, P.; Knop, Y.; Collman, J. P. *J. Am. Chem. Soc.* **1995**, *117*, 11721−11729.
(54) Scheidt, W. R.; Lee, Y. J. *Struct. Bonding (Berlin)* **1987**, *64*, 1−70.

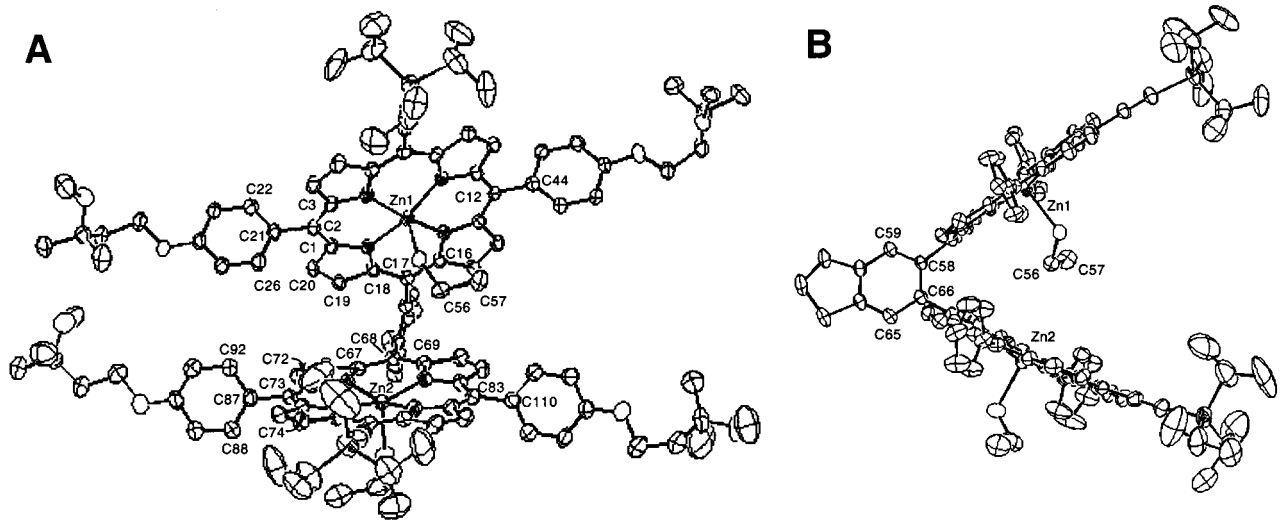

Figure 1. ORTEP representations of compound **9·(EtOH)$_2$** with thermal ellipsoids at 30% probability. (A) View down the indanyl bridge; (B) view orthogonal to the indanyl plane. Phenyl group alkyl substituents have been omitted for clarity.

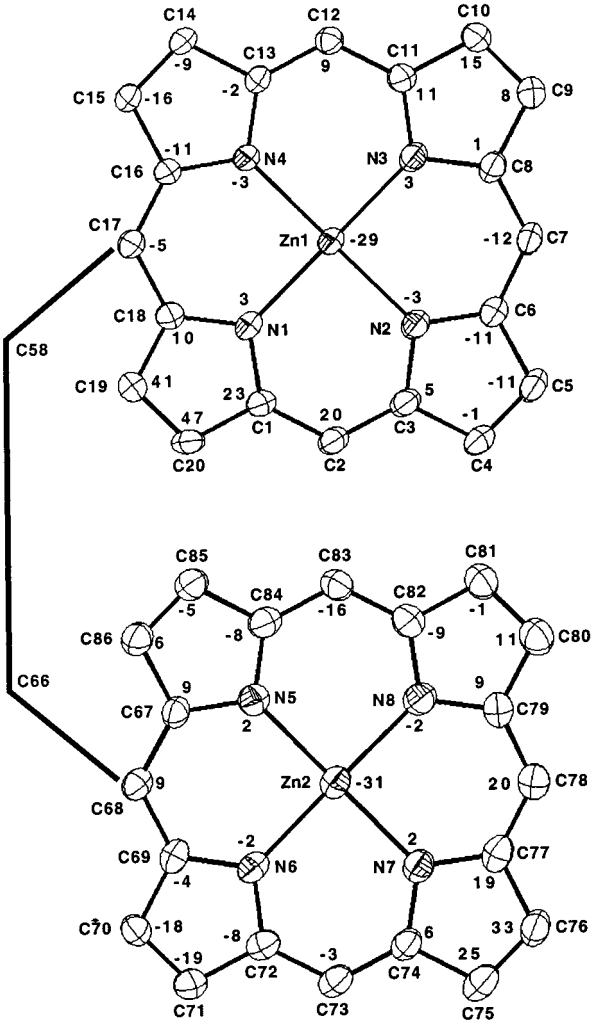

Figure 2. Diagrammatic representations of the porphyrin cores of **9·(EtOH)$_2$** illustrating the extent of the macrocycle saddling and ruffling distortions. The numbers adjacent to the atom labels signify the perpendicular displacements, in units of 0.01 Å, from the respective least squares plane as defined by the four porphyrin nitrogen atoms.

macrocycles is at the bridging *meso* positions; note that the C17−C68 separation is only 3.056(7) Å, well below the van

Table 2. Selected Bond Distances and Angles for **9·(EtOH)$_2$**

bond	distance, Å	bond	distance, Å
C2−C21	1.488(8)	C73−C87	1.494(9)
C12−C44	1.493(8)	C83−C110	1.490(9)
C17−C58	1.511(7)	C66−C68	1.505(8)
angle	**angle, deg**	**angle**	**angle, deg**
C2−C21−C22	121.9(6)	C73−C87−C88	121.1(7)
C2−C21−C26	121.1(6)	C73−C87−C92	122.1(7)
C17−C58−C59	117.9(5)	C68−C66−C65	117.5(6)
C17−C58−C66	123.4(5)	C68−C66−C58	122.9(5)
dihedral	**angle, deg**	**dihedral**	**angle, deg**
C1−C2−C21−C22	81.4(8)	C72−C73−C87−C88	77.6(8)
C3−C3−C21−C22	100.8(7)	C74−C73−C87−C88	101.1(8)
C16−C17−C58−C66	64.4(5)	C67−C68−C66−C58	75.8(6)
C18−C17−C58−C66	110.5(6)	C69−C68−C66−C58	108.4(6)

der Waals contact distance (3.40 Å).[55] Interestingly, an additional close interporphyrin contact exists between the C19 and C70 β-carbon atoms; these nuclei are separated by only 3.143(7) Å, and drive the anomalously large average perpendicular displacements (0.44 Å) observed at the C19 and C20 β carbons of **9·(EtOH)$_2$**'s Zn1 macrocycle.

The origin of the sub-van der Waals separation between the C19 and C70 β-carbons derives likely from steric interactions caused by the orientation of the ethanol moiety bound within the pocket of the cofacial bis[(porphinato)-zinc(II)] complex. Ethanol carbon atoms C56 and C57 are suspended 3.476(6) and 3.820(8) Å, respectively, above the N4 plane of the Zn2 macrocycle; note that the C56 methylene carbon of the Zn1-ligated ethanol lies above the N5−C84 bond (nonbonded distances: C56−N5, 3.553(9) Å; C56−C84, 3.613(8) Å). This interaction augments the $C_{\alpha}-C_{meso}-C_{5-indanyl}-C_{6-indanyl}$ dihedral angle (C16−C17−C58−C66) involving the Zn1 macrocycle, with respect to the analogous C67−C68−C66−C58 dihedral entailing the Zn2 porphyrin ring (Table 2), resulting in an asymmetric tilting of the Zn1 (64°) and Zn2 (76°) porphyrin least squares planes relative

(55) Pauling, L. *The Nature of the Chemical Bond*, 3rd ed.; Cornell University Press: Ithaca, NY, 1960.

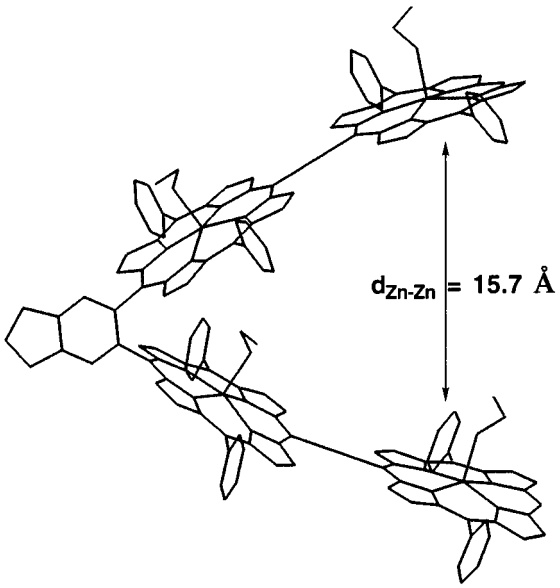

Figure 3. Molecular model of compound **2·(EtOH)$_4$** generated from the CaChe MM2 computational package and data obtained from the X-ray crystallographic structure of **9·(EtOH)$_2$**.

to the indanyl bridge least squares plane. The marked 4.16 Å lateral shift, coupled with (i) the significant observed atomic perpendicular displacements from the macrocycle least squares planes and (ii) the asymmetric tilting of the two (porphinato)zinc(II) units with respect to the indanyl bridge, serve to further illustrate the flexibility inherent to the 1,2-phenylene-based porphyrin-to-porphyrin linkage topology and the ease by which small molecules can be accommodated within the cavities of such cofacial bis(porphyrin) ligand frameworks.[33]

The X-ray crystallographic data obtained for **9·(EtOH)$_2$** can be utilized to estimate a typical distance that separates the porphyrin macrocycles appended via ethyne groups to the cofacial bis[(porphinato)metal] core of compound **2** in coordinating solvent. The Si−Si separation distance between the two peripheral TIPS groups in **9·(EtOH)$_2$** is 13.81 Å; simple replacement of each TIPS group with a 5′-(porphinato)zinc(II) unit within a molecular mechanics computational package[56] approximates a Zn−Zn separation of 15.7 Å between the central metal ions of the outer porphyrin rings (Figure 3). This analysis highlights the fact that supplemental π-cofacial interactions are essentially absent between the outer porphyrin rings of **2** in an open "Pac-Man" conformation and suggests that the observed electrooptic perturbations manifest in **2** relative to simple 1,2-phenylene-bridged bis[(porphinato)metal] compounds (e.g., **11**; vide infra) in coordinating solvents arise solely from substituent effects inherent to the (5-ethynylporphinato)zinc(II) moiety.

NMR Spectroscopy. The open conformation of **2** was confirmed via ^{1}H NMR experiments. Figure 4 highlights the resonances spanning the 7.0−10.5 ppm spectral domain for compounds **7**, **9**, and **2**. The ^{1}H NMR chemical shifts corresponding to the *ortho* and *meta* protons of the porphyryl 5- and 15-aryl substituents (labeled $H_{(o)}$ and $H_{(m)}$) are key indicators of the relative proximity of the porphyrin rings in cofacial orientations. Note that these signals appear as doublets for compound **7** (δ = 8.1 and 7.3 ppm; Figure 4A). In the analogous compound **9** spectrum (Figure 4B), the inequivalence of the $H_{(o)}$ and $H_{(m)}$ aryl protons that point toward and away from the cofacial pocket is clearly apparent: the $H_{(o)}$ resonances shift upfield and are split into two multiplets (labeled $H_{(o)in}$ and $H_{(o)out}$), while the *meta*-phenyl resonances shift upfield and appear as a closely overlapping pair of multiplets (labeled $H_{(m)in}$ and $H_{(m)out}$).

These characteristic shifts for the *o*-phenyl protons of **7** and **9** can be used to discern basic solution structural features of **2**. Note that the ^{1}H NMR spectrum for **2** (Figure 4C) evinces a simple doublet at δ = 8.15 ppm and multiplets at δ = 7.95 and 7.65 ppm that integrate in a 2/1/1 ratio: these spectral signatures correspond to the respective *o*-phenyl proton resonances observed for bis[(porphinato)zinc(II)] species **7** and **9**. These data show that **2** possesses two inequivalent pairs of porphyryl units: one set of these signals corresponds to the $H_{(o)}$ resonances for the closely spaced 1,2-phenylene-bridged bis[(porphinato)zinc(II)] core, while the second set delineates a pair of terminal porphyrin moieties that are separated by a distance sufficiently large such that the macrocycle ring currents do not significantly perturb aryl ring chemical shifts relative to the compound **7** benchmark. In this regard, two other compound **2** spectral features deserve comment: (i) the substantial distance between the outer porphyryl rings cannot derive from an extensive lateral shift,[54] as the β proton resonances reflect a plane of symmetry defined by the indanyl bridge, and (ii) the distinct resonance pattern between 9.0 and 10.5 ppm denotes two chemically equivalent *meso*-to-*meso* ethyne-bridged bis[(porphinato)zinc(II)] scaffolds.[25]

Electronic Absorption Spectroscopy. Electronic spectral features of tris- and tetrakis[(porphinato)zinc(II)] complexes **1** and **2** are consistent with their solution structures elucidated by NMR methods. Figure 5A,B displays reference spectra for the cofacial 1,2-phenylene-bridged and linear *meso*-to-*meso* ethyne-linked bis[(porphinato)zinc(II)] species **11** and **10**, respectively; the electronic structural characteristics of these classes of coupled bis(porphyrin) systems have been discussed previously.[25−27,57,58] With respect to compound **11**, note that an optical hallmark of the cofacial porphyrin structural motif is the presence of a B-state exciton band that is intensified and blue shifted relative to the Soret transition of an appropriate reference monomeric porphyrin. Consistent with this, the 411 nm band of compound **11** (Figure 5A) is observed to lie 634 cm^{-1} higher in energy with respect to the B-band transition for 5-phenyl-6-[(5′-10′,20′-di[4-(3-methoxy-3-methylbutoxy)phenyl]porphinato)zinc(II)]indane (**12**) (Figure 6A).

As evidenced in Figure 5C,E, the key spectral signatures that delineate cofacial bis(porphyrin) structures are also manifest in ethyne-bearing precursor structures **7** and **8**. Elaboration of **7** and **8** into supermolecular structures **1** and

(56) *Molecular Mechanics*, CaChe v. 4.5; CaChe Scientific: Beaverton, OR, 2000.

(57) Chang, C. K. *Adv. Chem. Ser.* **1979**, *173*, 162−177.
(58) Osuka, A.; Nakajima, S.; Maruyama, K. *J. Org. Chem.* **1992**, *57*, 7355−7359.

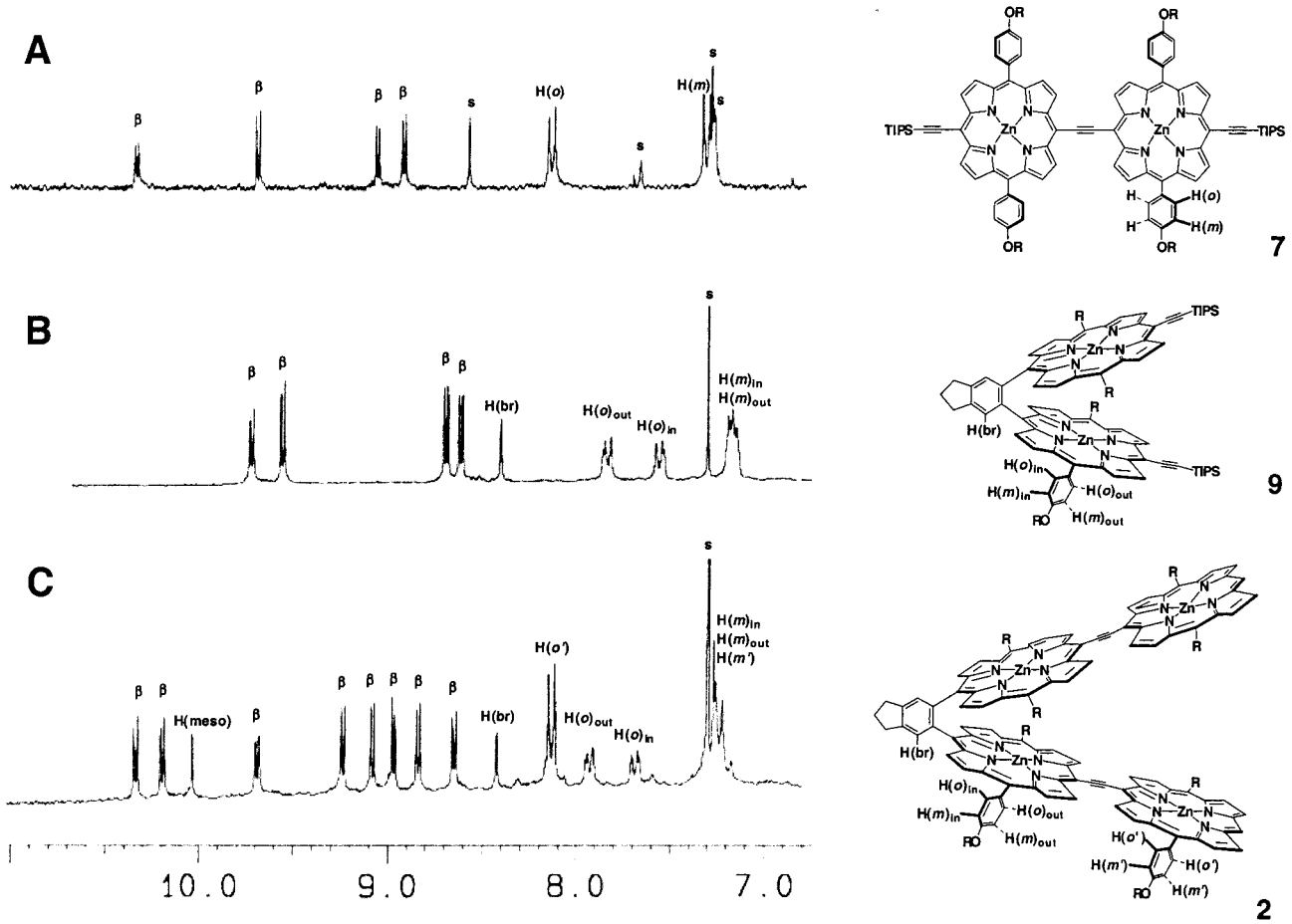

Figure 4. 250 MHz ^{1}H NMR spectra of (A) **7**, (B) **9**, and (C) **2** in 50/1 $CDCl_3/d_5$-pyridine spanning the 11.0−6.8 ppm spectral window. S = solvent peak.

2 gives rise to species that display electronic spectral characteristics of both cofacial and *meso*-to-*meso* ethyne-linked oligo[(porphinato)zinc(II)] compounds (Figure 5D,F). The optical spectrum of compound **1**, for example, shows an *intense* transition at 411 nm (ϵ = 275 500 M^{-1} cm^{-1}), a wavelength identical to that observed for **11**'s allowed B-state exciton band (Figure 5A), suggesting a cofacial exciton coupling energy similar to that manifest in the dimeric reference compound; **1**'s Q-state manifold spectral features, as well as the energetic splitting between its prominent B-state absorptions (3288 cm^{-1}), are reminiscent of those observed for *meso*-to-*meso* ethyne-bridged **10**.[25,26]

The electronic absorption spectrum of tetrakis[(porphinato)zinc(II)] complex **2** displays the gross spectral features of a *meso*-to-*meso* ethyne-bridged [(porphinato)zinc(II)] dimer. Comparison of the Figure 5F spectrum with that for the reference compound, [(5-15-[5″-6″-(phenyl)indanyl)]-10,20-di[4-(3-methoxy-3-methylbutoxy)phenyl]porphinato)-zinc(II)]-[(5′-10′,20′-di[4-(3-methoxy-3-methylbutoxy)phenyl]-porphinato)zinc(II)]ethyne (**13**, Figure 6B), shows a striking correspondence of the λ_{max} values for the key optical transitions. The effects of cofacial exciton coupling in **2**, however, are readily apparent, causing an increase in oscillator strength of the high energy B-state transition manifold centered at 419 nm and a general broadening of the visible regime absorptive signature relative to that manifest for **13**. Note that the full-width-at-half-maximum (fwhm) of the B-band region (∼360−525 nm) increases by 1133 cm^{-1} in **2** (5399 cm^{-1}) relative to **13** (4266 cm^{-1}); furthermore, simplex fitting shows that the fwhm of **2**'s low energy Soret transition envelope centered at 479 nm has increased substantially (fwhm = 1045 cm^{-1}) with respect to the analogous low energy B-state spectral domain of **13** (fwhm = 438 cm^{-1}).

Electrochemical Data. Potentiometric data for reference monomer **12**, reference dimers **11** and **13**, as well as compounds **1** and **2** are summarized in Table 3. As expected,[25,59] cyclic voltammetric experiments show that the first oxidation processes for both cofacial and *meso*-to-*meso* ethyne-bridged bis[(porphinato)zinc(II)] systems porphyrin dimers are split into two one-electron steps. Typical of bis-[(porphinato)metal] compounds featuring close interplanar contacts,[59,60] the initial step of the first oxidation process for cofacial reference dimer **11** is destabilized relative to that determined for benchmark porphyrin monomer **12**. Such redox behavior derives from the filled $\pi-\pi$ interactions characteristic of two closely spaced aromatic macrocycles.[59] Following removal of the first electron from such cofacial bis[(porphinato)zinc(II)] compounds, electronic delocalization serves to stabilize the second step of **11**'s first oxidation

(59) Le Mest, Y.; L'Her, M.; Hendricks, N. H.; Kim, K.; Collman, J. P. *Inorg. Chem.* **1992**, *31*, 835−847.
(60) Osuka, A.; Nakajima, S.; Nagata, T.; Maruyama, K.; Toriumi, K. *Angew. Chem., Int. Ed. Engl.* **1991**, *30*, 582−584.

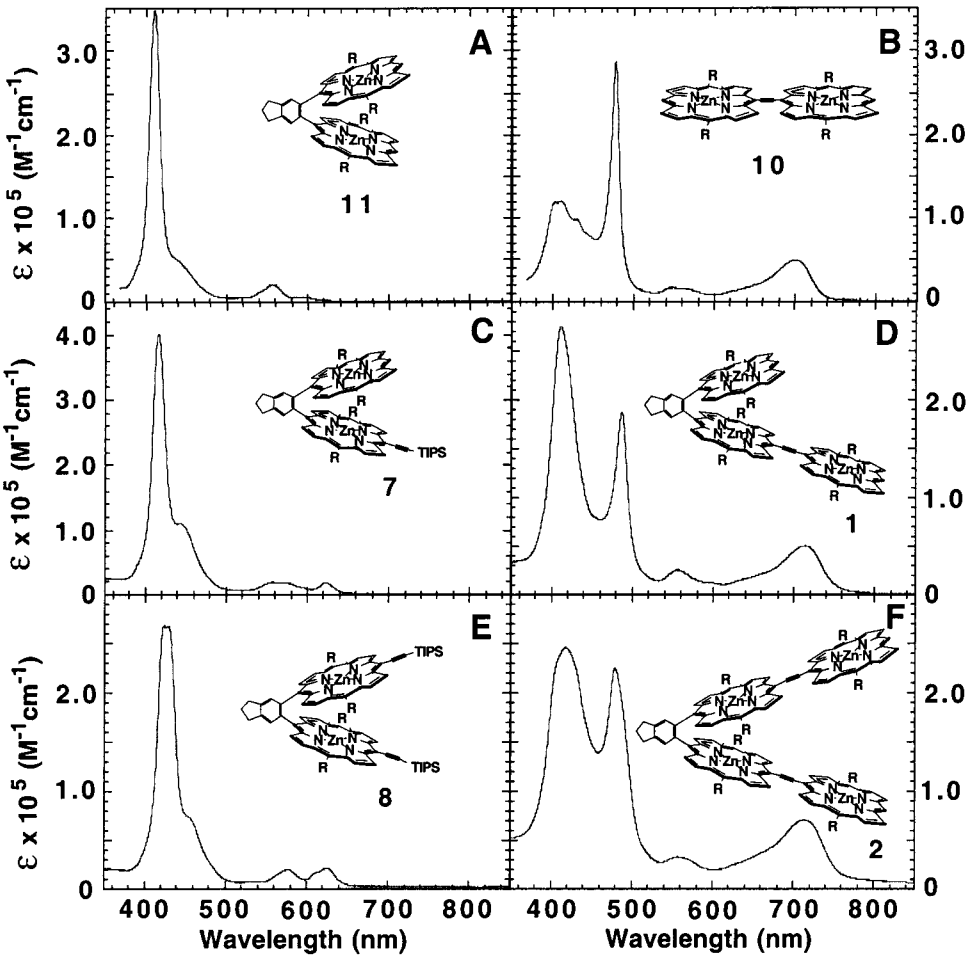

Figure 5. Electronic absorption spectra of (A) **11**, (B) **10**, (C) **7**, (D) **1**, (E) **8**, and (F) **2** in THF.

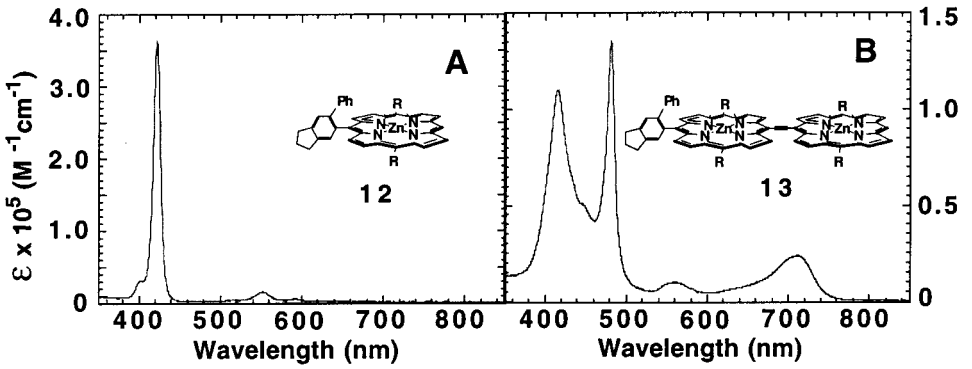

Figure 6. Electronic absorption spectra of (A) **12** and (B) **13** in THF.

process relative to the $E_{1/2}$(ZnP/ZnP$^+$) potential determined for **12**.

The first oxidation process for tris[(porphinato)zinc(II)] **1** is split into two observable steps, with a redox splitting (215 mV) reminiscent of that manifest for *meso*-to-*meso* ethyne-bridged **13**. The first step, one-electron (1e) in nature, occurs at +555 mV and is shifted cathodically 15 mV with respect to **13**'s initially observed 1e oxidation potential. The second step of **1**'s first oxidation process is 2e in nature and occurs at a potential (770 mV vs SCE) intermediate between those determined for the second 1e redox steps of the first oxidation processes of the cofacial (**11**) and ethyne-bridged (**13**) bis-[(porphinato)zinc(II)] benchmarks (Table 3). The anodic cyclic voltammetric responses observed for the tetrakis-[(porphinato)zinc(II)] complex **2** are similar to those observed for **1** (Table 3); notably, the first step of the first oxidation process for **2** is 2e in nature and is shifted cathodically 15 mV relative to **1**'s initial oxidation potential. These potentiometric data for compounds **1**, **2**, and **11**−**13** thus show (i) that the extensive π-conjugation enabled by the *meso*-to-*meso* ethyne-bridged porphyrin-to-porphyrin linkage topology, which gives rise to substantial redox splitting, determines essentially the anodic current versus potential profiles observed in the cyclic voltammetric studies of compounds

Table 3. Cyclic Voltammetric Data (mV)[a]

compound	ZnP/ZnP$^+$	ZnP$^+$/ZnP^{2+}	ZnP/ZnP$^-$
12	705 (1)	1010 (1)	−1495 (1)
11	620 (1), 750 (1)	1070 (1), 1250 (1)	−1720 (2)
13	570 (1), 790 (1)	1255 (2)	−1235 (1), −1335 (1)
1	555 (1), 770 (2)	1270 (3)	−1420 (3)
2	540 (2), 770 (2)	1280 (4)	−1425 (4)

[a] Experimental conditions: solvent = benzonitrile; [porphyrin] = 1 mM; [$TBAClO_4$] = 0.1 M; scan rate = 100−1000 mV/s; reference electrode = Ag wire. $E_{1/2}$ values reported are relative to SCE; the ferrocene/ferrocenium redox couple (0.43 V vs SCE, benzonitrile) was used as an internal standard. The number in parentheses following each potential denotes the number of electrons involved in that redox process.

1 and **2**, and (ii) while both porphyrin−porphyrin π-cofacial and π-conjugative electronic interactions deriving from the ethynyl linkage topology serve to destabilize the HOMO of the composite supermolecular complex, the extent to which the HOMOs of **1** and **2** are further destabilized relative to **13** by their respective supplemental π-cofacial interactions is only on the order of 10−30 mV.

The cathodic electrochemistry observed for reference bis[(porphinato)zinc(II)] compounds **11** and **13** shows that these species display the signature current−potential responses for their respective first reduction processes noted previously for cofacial and *meso*-to-*meso* ethyne-bridged bis[(porphinato)zinc(II)] structures.[25,59] It is important to appreciate that while the cofacial porphyrin motif destabilizes the LUMO, giving rise to $E_{1/2}$(ZnP$^-$/ZnP) values that are substantially lower than those determined for appropriate benchmark (porphinato)zinc(II) compounds, a *meso*-to-*meso* ethyne-bridging linkage topology stabilizes significantly the LUMO with respect to that of its simple (porphinato)zinc(II) building block. For the compounds listed in Table 3, it can be seen that the magnitudes of these electronic perturbations are approximately equal and opposite. Note that the potential of cofacial **11**'s initial 2e reduction is suppressed 225 mV relative to that observed for monomer **12**, while the potential of the initial 1e step of *meso*-to-*meso* ethyne-bridged **13**'s first cathodic redox process is increased by 260 mV relative to the compound **12** benchmark. These electronic effects that derive from these two classes of porphyrin−porphyrin linkage motifs apparently conspire in compounds **1** and **2** to give rise to cathodic cyclic voltammetric responses that are multielectron in nature at potentials intermediate between those determined for the initial reductive events of the cofacial and *meso*-to-*meso* ethyne-bridged bis[(porphinato)zinc(II)] benchmarks **11** and **13** (Table 3).

Conclusions

Sequential cobalt-catalyzed [2+2+2] cycloadditions and palladium-catalyzed cross-coupling reactions provide access to supermolecular structures that manifest both classic structural motifs that have been demonstrated to provide substantial electronic communication between (porphinato)metal centers: face-to-face organization and direct macrocycle-to-macrocycle linkage via cylindrically π-symmetric bridging moieties. We report two archetypal multiporphyrin structures that manifest both 1,2-phenylene- and ethyne-based *meso*-to-*meso* linkage topologies; structural, spectroscopic, and potentiometric properties of these systems show that (i) the 1,2-phenylene-bridged cofacial bis[(porphinato)zinc(II)] component of these systems can adopt the open conformation required for substrate binding and (ii) ethynyl(porphinato)metal moieties appended directly to either macrocycle of the cofacial porphyrin core are strongly coupled to this unit. We posit that the now established combination of these structural elements holds promise for the elaboration of new classes of redox catalysts competent to both bind small molecule substrates and effect concerted, multielectron redox transformations.

Acknowledgment. This work was supported in part by the MRSEC Program of the National Science Foundation (DMR00-79909) and the Office of Naval Research (N00014-98-1-0187). M.J.T. acknowledges the Camille and Henry Dreyfus Foundation for a research fellowship. J.T.F. thanks the International Precious Metals Institute (IPMI) for a graduate student research award. The structure of compound **9** was determined by Dr. Patrick Carroll (X-ray Facility, Department of Chemistry, University of Pennsylvania).

Supporting Information Available: Characterization data and detailed syntheses of compounds **12**−**17**, tables of crystal data, and a labeled ORTEP diagram (22 pages PDF); X-ray crystallographic file for **9** (CIF format). This material is free of charge via the Internet at http://pubs.asc.org.

IC010871P